

# Neurons in V1, V2, and PMLS of Cat Cortex Are Speed Tuned But Not Acceleration Tuned: The Influence of Motion Adaptation

N.S.C. Price, N. A. Crowder, M. A. Hietanen and M. R. Ibbotson

*J Neurophysiol* 95:660-673, 2006. First published Sep 21, 2005; doi:10.1152/jn.00890.2005

**You might find this additional information useful...**

---

This article cites 58 articles, 28 of which you can access free at:

<http://jn.physiology.org/cgi/content/full/95/2/660#BIBL>

Updated information and services including high-resolution figures, can be found at:

<http://jn.physiology.org/cgi/content/full/95/2/660>

Additional material and information about *Journal of Neurophysiology* can be found at:

<http://www.the-aps.org/publications/jn>

---

This information is current as of February 3, 2007 .

## Neurons in V1, V2, and PMLS of Cat Cortex Are Speed Tuned But Not Acceleration Tuned: The Influence of Motion Adaptation

N.S.C. Price, N. A. Crowder, M. A. Hietanen, and M. R. Ibbotson

Visual Sciences, Research School of Biological Sciences, Australian National University, Canberra, ACT, Australia

Submitted 25 August 2005; accepted in final form 20 September 2005

**Price, N.S.C., N. A. Crowder, M. A. Hietanen, and M. R. Ibbotson.** Neurons in V1, V2, and PMLS of cat cortex are speed tuned but not acceleration tuned: the influence of motion adaptation. *J Neurophysiol* 95: 660–673, 2006. First published September 21, 2005; doi:10.1152/jn.00890.2005. We studied neurons in areas V1, V2, and posteromedial lateral suprasylvian area (PMLS) of anesthetized cats, assessing their speed tuning using steps to constant speeds and acceleration and deceleration tuning using speed ramps. The results show that the speed tuning of neurons in all three cortical areas is highly dependent on prior motion history, with early responses during speed steps tuned to higher speeds than later responses. The responses to speed ramps are profoundly influenced by speed-dependent response latencies and ongoing changes in neuronal speed tuning due to adaptation. Acceleration evokes larger transient and sustained responses than subsequent deceleration of the same rate with this disparity increasing with ramp rate. Consequently, there was little correlation between preferred speeds measured using speed steps, acceleration or deceleration. From 146 recorded cells, the proportion of cells that were clearly speed tuned ranged from 69 to 100% across the three brain areas. However, only 13 cells showed good skewed Gaussian fits and systematic variation in their responses to a range of accelerations. Although suggestive of acceleration coding, this apparent tuning was attributable to a cell's speed tuning and the different stimulus durations at each acceleration rate. Thus while the majority of cells showed speed tuning, none unequivocally showed acceleration tuning. The results are largely consistent with an existing model that predicts responses to accelerating stimuli developed for macaque MT, which showed that the responses to acceleration can be decoded if adaptation is taken into account. However, the present results suggest future models should include stimulus-specific adaptation and speed-dependent response latencies.

### INTRODUCTION

Studies of visual motion sensitivity at the neuronal level typically use stimuli with fixed size, contrast, direction, and speed. However, in the natural environment, these parameters continually change, making it important to understand how individual neurons represent stimulus parameters as they change. For example, although many studies have made it clear that neurons can code the change in position of an object, or its speed (e.g., Movshon 1975), it is not clear if the same neurons specifically code changes in an object's speed or its acceleration. In addition to problems associated with representing changing visual stimuli, the responses of most motion-sensitive neurons adapt, showing a decline in spiking rate over time when exposed to sustained motion (e.g., retina, Barlow and Hill 1963; cortex, Vautin and Berkley 1977). This presents difficulties when interpreting a neuron's response to changing

parameters because both the stimulus and the neuron's responsiveness to that stimulus are dynamically varying.

There is little evidence that adaptation is caused by neural fatigue because its strength is not directly related to firing rate (Vidyasagar 1990). Rather, the rate of physiological adaptation is dependent on a range of stimulus parameters including contrast (Ohzawa et al. 1982, 1985), direction (Giaschi et al. 1993; Petersen et al. 1985), and temporal frequency (Maddess et al. 1988). This is supported by human psychophysical work showing that the rates of adaptation and recovery after motion adaptation are also stimulus dependent (Bex et al. 1999; Keck and Pentz 1977; Lorenceau 1987; Smith 1985). Many reports suggest that adaptation is a purposeful or beneficial mechanism (for review, Ibbotson 2005b). For example, contrast adaptation is hypothesized to act as a gain control mechanism, increasing the sensitivity of a neuron to contrasts near those to which it has been recently exposed (Ohzawa et al. 1985). Further, Bonds (1991) showed that systematic, stepped increases and decreases in the contrast of a moving grating lead to response hysteresis in simple and complex cells in cat striate cortex. Spiking rates evoked by a stimulus of a specific contrast are higher if the stimulus is preceded by a low contrast than if it is preceded by a high contrast. Contrast adaptation is thus thought to be a mechanism allowing high-contrast discrimination abilities across a broad range of contrasts despite the constraints imposed by the limited signaling bandwidth associated with a spike-rate code (Albrecht et al. 1984; Bonds 1991; Ohzawa et al. 1985).

Given the hysteresis inherent in responses to changing contrasts, how does the visual system address the problem of changing speeds? We describe three functional possibilities here: first, the visual system may be explicitly sensitive to stimulus acceleration, with neurons displaying acceleration tuning in the same way that motion-sensitive neurons are tuned for direction, temporal frequency, spatial frequency, or speed. Second, it is possible that the combination of neuronal adaptation and a changing stimulus may degrade a neuron's ability to accurately code stimulus parameters. This would present serious problems for the visual system because it would deal poorly with the ever-changing motion associated with the real world. Finally, although not explicitly coding stimulus acceleration, it may still be possible to resolve the stimulus speed at each point in time from a neuron's instantaneous responses. This could occur if the neuron's preferred speed is preserved even when presented with changing stimuli, or if knowledge

Address for reprint requests and other correspondence: M. R. Ibbotson, Visual Sciences, Research School of Biological Sciences, Australian National University, Canberra, ACT, Australia 2601 (E-mail: Michael.Ibbotson@anu.edu.au).

The costs of publication of this article were defrayed in part by the payment of page charges. The article must therefore be hereby marked "advertisement" in accordance with 18 U.S.C. Section 1734 solely to indicate this fact.

about the neuron's adaptation state is used to determine the cell's new preferred speed. Thus adaptation may enhance the coding of changing scenes, ensuring that the visual system maintains optimal sensitivity to new stimuli.

Psychophysical studies overwhelmingly suggest that human observers are poor at processing acceleration (Snowden and Braddick 1991; Werkhoven et al. 1992), despite the ability to reliably distinguish speed differences of <5% (McKee 1981). Thus in tasks requiring the detection or distinguishing of acceleration and deceleration, it is likely that observers simply compare stimulus velocities at two points in time rather than maintaining a continuous internal representation of acceleration (Brouwer et al. 2002; Watamaniuk and Heinen 2003). The physiological and psychophysical data, combined with arguments that the initiation and maintenance of smooth pursuit eye movements is partially dependent on acceleration information (Krauzlis and Lisberger 1994; Lisberger et al. 1987), suggest that while the visual system may analyze stimulus acceleration, the information does not reach the perceptual level.

Physiological studies have demonstrated acceleration sensitivity in neurons that contribute to smooth pursuit and optokinetic eye movements in a range of midbrain and brain stem areas including: neurons in macaque dorsolateral pontine nucleus and nucleus reticularis tegmenti pontis (DLPN and NRTP) (Ono et al. 2005; Suzuki et al. 2003); parafoveal cells in the primate pretectal nucleus of the optic tract (NOT) (Das et al. 2001); and pretectal neurons in the pigeon nucleus lentiformis mesencephali (LM) (Cao et al. 2004). Notably, in the primate, area MT is a primary source of motion information to the NOT and NRTP, yet it shows no acceleration sensitivity at the single neuron level (Lisberger and Movshon 1999; Price et al. 2005). However, the firing rate of neurons in MST, which receives inputs from MT and subsequently projects to the DLPN, shows some dependence on acceleration in the retinal slip signal (Takemura et al. 2001). The acceleration sensitivity of motion sensitive neurons in areas V1 and V2 has not been studied in any species, nor is it clear how the responses to acceleration can be decoded to accurately represent stimulus speed.

In the cat, cortical analysis of motion is initially performed simultaneously and collaboratively by a range of interconnected regions including V1 (area 17), V2 (area 18), and posteromedial lateral suprasylvian area (PMLS), the posteromedial lateral suprasylvian cortex (Dinse and Kruger 1994; Katsuyama et al. 1996; Vajda et al. 2004). The majority of neurons in these areas respond better to moving rather than stationary stimuli and have strong orientation or direction preferences and spatiotemporal-frequency or speed tuning (e.g., Morrone et al. 1986; Movshon 1975; Movshon et al. 1978). We studied the responses of neurons in V1, V2, and PMLS in anesthetized cats to constant speed steps and linear speed ramps comprising constant rates of acceleration and deceleration. In individual neurons, we found no strong evidence for acceleration tuning, unlike their characteristic speed and direction tuning. We suggest that neuronal adaptation may account for our findings that responses to acceleration were larger than responses to the corresponding deceleration rate. Adaptation may also explain why predictions of the cell's preferred speed based on responses to speed ramps were poorly correlated with preferred speeds predicted from responses to speed steps.

## METHODS

Experimental procedures complied with the guidelines of the Australian National Health and Medical Research Council and were approved by the Animal Experimentation Ethics Committee of the Australian National University.

### *Physiological preparation*

Data were collected from nine adult cats of either sex weighing 2.8–4.2 kg in experiments lasting 4–5 days. Animals were initially anesthetized with intramuscular ketamine HCl and xylazine HCl (20 and 1 mg/kg, respectively; Ilium, Smithfield, NSW, Australia) to allow the trachea and right cephalic vein to be cannulated. Neuro-muscular blockade was then induced with an intravenous injection of 20 mg gallamine triethiodide (Flaxedil; Sigma, St. Louis, MO) in 3 ml of Hartmann's solution and maintained with continuous intravenous infusion of Flaxedil at a rate of  $10 \text{ mg} \cdot \text{kg}^{-1} \cdot \text{h}^{-1}$  in a 1:1:2 mixture of Hartmann's solution, 5% glucose, and 8% amino acid solution. With the initiation of paralysis, anesthesia was maintained by ventilation with a mixture of gaseous halothane (0.5% during electrophysiological recording and 1–1.5% during surgery) and a 2:1 ratio of  $\text{N}_2\text{O}$  and  $\text{O}_2$ . Expired  $\text{CO}_2$  was monitored continuously and maintained at 3.5–4% by adjusting the breath rate or stroke volume of the pulmonary pump. Heart rate was monitored continuously, and body temperature was maintained at 38°C with an electric heating blanket. We administered daily intramuscular injections of 1 ml Clavulox (140 mg/ml amoxicillin and 35 mg/ml clavulanic acid; Pfizer, West Ryde, NSW, Australia), 1 ml dexamethasone sodium phosphate (5 mg/ml; Ilium) and atropine (0.05 mg/kg; Apex Laboratories, Somersby NSW, Australia).

The corneas were protected with zero-power rigid gas-permeable contact lenses. Pupils were dilated and accommodation was paralyzed with 1% atropine sulfate eye-drops (Sigma) while the nictitating membranes were retracted with 0.01% phenylephrine HCl eye-drops (Sanofi-Synthelabo). Corrective lenses were used to focus the eyes at a distance of 57 cm in front of the animal. Artificial pupils (3 mm diam) were placed in front of each eye to reduce spherical aberration. The locations of the optic disc and area centralis of each eye were plotted daily by reverse ophthalmoscopy to ensure the stability of paralysis and check for eye drift.

Each animal's head was held in a stereotaxic frame during surgery and recording. Recordings in V1 and V2 were made in different animals from those used to record from PMLS. To access V1 and V2 in the right hemisphere, we used vertical electrode penetrations through a craniotomy from 0 to 8 mm posterior to interaural zero and from 2 mm left of the midline to 8 mm right of the midline. PMLS was accessed using penetrations perpendicular to the banks of the suprasylvian sulcus, at an angle of 30°. A craniotomy from 4 mm posterior to 6 mm anterior to interaural zero and from 10 to 18 mm lateral to the midline was used. Extracellular recordings were made with lacquer coated tungsten microelectrodes (Fredrick Haer, Bowdoinham, ME). Signals were amplified and filtered then acquired at 25 kHz with a 1401plus interface and Spike2 software (Cambridge Electronic Design, Cambridge, UK). The extracellular recording was also passed through a Schmitt trigger, producing TTL pulses at the time of each action potential that were used by Spike2 to generate on-line peri-stimulus time histograms (PSTHs) of the spiking activity. Off-line, isolations were checked using the Wavemark function in Spike2.

### *Stimuli*

After isolating a neuron, its dominant eye, receptive field location and spatial structure were qualitatively determined using a hand-driven light or dark bar. Only the dominant eye was tested quantitatively, using custom visual stimuli produced by a VSG Series 2/5 stimulus generator (Cambridge Research Systems, Cambridge, UK),

and presented on a gamma-corrected monitor (Eizo T662-T, 100 Hz, 57 cd/m<sup>2</sup> mean luminance, 1,024 × 768 pixels) at a viewing distance of 57 cm. Using grating stimuli we determined the location and size of each neuron's classical receptive field, as well as its direction tuning. Neurons in V1 and V2 were classified as simple or complex qualitatively based on the separability of receptive field regions sensitive to light-on and light-off and quantitatively by calculating the quotient of the amplitude of oscillations at the stimulus temporal frequency ( $F_1$ ) and the mean response amplitude ( $F_0$ ) (Ibbotson et al. 2005; Skottun et al. 1991). For the quantitative tests, the grating was of the neuron's preferred size and spatial frequency, moving in its preferred direction at its preferred temporal frequency.

The responses to constant speed steps and linear speed ramps were tested using stimuli moving in a cell's preferred direction and positioned inside the cell's classical receptive field. Two aperiodic stimuli were used: first, a random texture pattern of black and white 0.8° squares, rotated so that the orientation of the squares aligned with the preferred orientation of the cell (Fig. 1*F*); second, an aperiodic grating or smoothed random noise stimulus (Fig. 1*G*). In total, 40 cells were tested with both stimuli, and no significant differences were found between the responses. Hence we do not specify which stimulus was used for each cell. The smoothed noise stimulus was generated by convolving a 20-pixel half-sinewave with a 1,024-pixel seed vector containing values uniformly distributed between 0 and 1. The convolution was performed three times, with the resulting vector used to define the luminance of stripes aligned with the cell's preferred orientation. The convolution operations provide a stimulus with low-pass spatial frequency content, with little or no power in spatial

frequencies >1 cpd. The spatial frequency content of these aperiodic stimuli is known to cover the sensitivity range of most cells in V1, V2, and PMLS (Casanova et al. 1995; Hamada 1987; Merabet et al. 2000; Morrone et al. 1986; Movshon et al. 1978; Zumboich and Blakemore 1987). However, as in previous studies, we found that only ~70–80% of neurons in each area responded to the motion of visual noise or random stripes (Casanova et al. 1995; Hamada 1987; Merabet et al. 2000), and only the responses of these neurons are reported here.

Speed tuning was tested using steps in stimulus speed lasting 3 s. For each cell, 7–12 constant speeds in the range 0.5–240°/s were presented preceded and followed by a stationary stimulus for ≥1s. Responses to acceleration and deceleration were tested using linear speed ramps of variable duration but with a fixed plateau speed of 120 or 240°/s. These tests had symmetric speed profiles: stationary for 1 s; acceleration to the plateau speed; constant speed for 1 s; deceleration to 0°/s at the same rate as the acceleration period; stationary for 1s (see Fig. 6). Ramp rates of 30, 60, 80, 120, 240, 480, 960, and 2400°/s<sup>2</sup> taking from 0.1 to 4 s to reach the plateau speed were tested. For all stimuli, 8–32 repetitions were performed.

### Data analysis

Neuronal responses to individual stimulus repetitions were aligned relative to a synchronization pulse provided by the stimulus generation computer in the blanking interval prior to the first stimulus frame. A continuous estimate of spiking rate was found by representing responses as spike density functions (SDFs) with 1-kHz resolution generated by initially convolving a delta function at each spike arrival

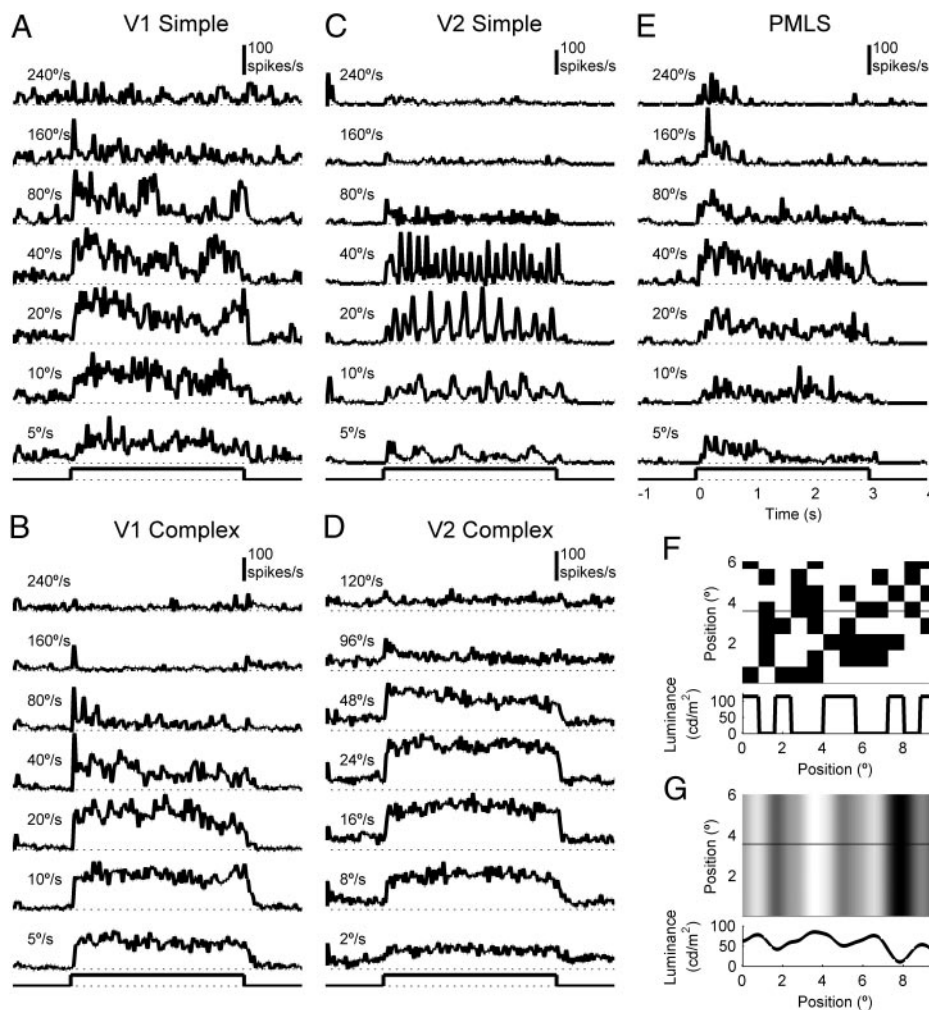


FIG. 1. Spike density functions (SDFs) associated with steps in stimulus speed lasting 3 s. Responses are shown for simple and complex cells from V1 (A and B), V2 (C and D), and a posteromedial lateral suprasylvian area (PMLS) cell (E). Each SDF is the average of the responses to 16 stimulus repetitions. For demonstration purposes, the stimulus for the V2 simple cell (C) did not have randomized start positions. As a result, bursts in spiking activity are evident for tests of 10–40°/s. However, for tests on the other cells, the start positions were randomized. . . . , 0 spikes/s level. The speed of the step in each test is marked to the left of each SDF. —, stimulus period, when the speed stepped from 0°/s to the test speed, and then returned to 0°/s. An 8 × 8° section of the random texture (F) and smoothed noise (G) stimulus are shown above a 1-dimensional luminance profile of each stimulus at the point marked by the horizontal line. The stimulus was always presented within a circular annulus matched to the cell's receptive field size.

time with a Gaussian window ( $\sigma = 3$  ms). SDFs were then calculated by averaging responses to individual stimulus presentations.

Response latencies were calculated using a Poisson-statistic method similar to that described by Maunsell and Gibson (1992). First, the spontaneous neuronal activity in the 500 ms of stationary pattern presentation before motion onset was fit with a Poisson distribution. From this fit, a threshold was determined from the rate below which the spontaneous spiking rate would be expected to lie for 99% of the time. The response latency was taken as the first time after stimulus onset when the SDF exceeded this threshold and stayed above the threshold for the subsequent 25 ms.

The responses to speed steps were calculated in two ways. First the sustained response was found by averaging the firing rate from 300 ms after motion onset to the end of motion. Second, the transient response was calculated using a sliding 24-ms window over the first 300 ms after motion onset, using 1-ms steps in the window start time. The cell's transient response was taken from the 24-ms window that gave the highest mean spiking rate. Sustained and transient responses to speed ramps were calculated using similar methods. The sustained response to a speed ramp was calculated by averaging the firing rate in a window of the same duration as the speed ramp, but delayed by the cell's latency at its preferred speed. The transient response to a speed ramp was determined by calculating the mean firing rate within all 24-ms windows during the latency-adjusted ramp period. The transient response was taken from the window giving the highest spiking rate and the time of the response peak was taken as the center of the window in which the firing rate peaked.

For each cell, the transient and sustained responses to speed steps and ramps were fit with a skewed-Gaussian function

$$R_x = R_{\max} \exp\left(-\left(\frac{\log(x/x_{\text{pref}})}{B + A\log(x/x_{\text{pref}})}\right)^2\right) + R_{\text{Spont}}$$

where  $R_x$  is the response at speed or acceleration  $x$ ;  $R_{\max}$  controls the amplitude;  $x_{\text{pref}}$  is the cell's preferred speed or acceleration, at which the peak spiking rate  $R_{\max}$  occurs;  $A$  controls the skew of the curve and  $B$  is the bandwidth.  $R_{\text{Spont}}$  is the measured spontaneous activity and was not allowed to vary as part of the least-squares fitting routine.

### Histology

At the end of recording sessions, electrodes were repeatedly moved up and down in the final track over a range of 50  $\mu\text{m}$ , always stopping at the same final depth. This generated a dense region of cell damage at the tip of the electrode, which provided a good marker of the final track depth without needing to damage the electrode tip by passing current through it. In three cats, a different electrode was also inserted 2–3 mm medial to the recording sites and electrolytic lesions (5–10 s, tip negative, 4  $\mu\text{A}$ ) were made at depths of 2, 4, and 6 mm below the brain surface. This allowed calibration for shrinkage produced by fixing the brain.

After placing lesions, animals were given a lethal dose of pentobarbitone sodium (120–180 mg depending on animal's weight) and immediately perfused with 0.9% saline followed by 10% formal saline. Brains were extracted and cryoprotected in sucrose (30% in 0.1 M PB) for 2–10 days. Frozen sections (45  $\mu\text{m}$  thick in the coronal plane) were collected and mounted on gelatin-coated slides before counterstaining for Nissl substance with 0.05% thionin. The tissue was then examined using light microscopy to confirm the locations of each cell within the expected brain region. The border between areas V1 and V2 was noted during recording when a marked shift in receptive field position occurred and was confirmed histologically using the increased thickness of layer 3 to distinguish the areas. Combined with the depth measurements recorded for each neuron we localized each cell within either areas V1, V2 or PMLS, but did not

rigorously determine the cortical layer of each cell by placing multiple microlesions.

### RESULTS

We recorded the responses of 146 cortical cells to aperiodic stimuli with speed profiles of either constant steps or linear ramps comprising constant acceleration and deceleration. The cells were distributed among three areas: 76 in V1 (13 simple, 63 complex); 27 in V2 (7 simple, 20 complex); and 43 cells in the PMLS. Complex cells were favored when recording from V1 and V2 because we found that they responded more strongly to our stimuli (see also Casanova et al. 1995). The results presented in the following text are divided into three main sections. First we assess each neuron's speed tuning and its dependence on adaptation (Figs. 1–4). Second, we assess each neuron's sensitivity to acceleration, comparing the responses to accelerations and decelerations of the same rate, and accelerations of different rates (Figs. 5–7). Finally, we assess the possibility of predicting a cell's preferred speed using the responses to speed ramps and conversely, predicting a cell's responses to speed ramps from the responses to speed steps (Figs. 8 and 9).

#### Responses to speed steps

The speed tuning of all cells was measured using 7–12 steps in speed from 0 to 240°/s, each lasting 3 s. The responses of V1 simple and complex cells, V2 simple and complex cells and a PMLS cell to these steps are shown as SDFs averaged from 16 presentations of each stimulus (Fig. 1). For speeds between 10 and 40°/s, clear bursts in spiking activity are evident in the SDFs for the V2 simple cell (Fig. 1C). These data are presented for comparative reasons because it was recorded using an aperiodic stimulus in which the start position was not randomized and the bursts are due to the stimulus having randomly spaced dark and light regions. Such oscillations were not usually evident in complex or PMLS cells because of their receptive field characteristics. To avoid this bursting activity and to be consistent across cell types, we randomized the start position of the stimuli across the 16 stimulus presentations (as presented in Fig. 1, A, B, D, and E). Despite these precautions, the responses of simple cells in both V1 and V2 were typically more variable over time than responses of complex or PMLS cells (e.g., Fig. 1A).

Most cells showed adaptation in their responses to motion, characterized by a large initial firing rate, followed by slow response decay to a sustained firing level. Some cells, like the V2 complex cell in Fig. 1D, showed little adaptation after motion onset, except at the higher speeds (upper SDFs). The magnitude of the transient response and subsequent sustained response were poorly correlated, as demonstrated by the response of a PMLS cell to a 160°/s step in speed (Fig. 1E). At this speed, a large initial response transient is evoked but subsequent motion fails to generate any response above the spontaneous firing level.

#### Transient and sustained speed tuning

To quantify a cell's speed tuning, we measured the *transient* and *sustained* responses to motion (see METHODS for details). The relative size of the transient and sustained responses can be

further used to quantify the level of neuronal adaptation at each speed. Speed tuning curves for the five cells shown in Fig. 1 are presented with the corresponding best fit skewed Gaussian (Fig. 2, A–E). Across the population of cells, skewed Gaussians provided excellent fits to the raw data with median  $R^2$  values of 0.90 and 0.96 for transient and sustained responses, respectively. The appropriateness of the skewed Gaussian fit was judged using an  $F$  test to compare the fit with that produced by a constant, speed-independent firing rate. The  $F$  test judging the appropriateness of the skewed Gaussian fit is later used to help indicate if a cell shows speed tuning—if a cell's response to motion is independent of stimulus speed, it cannot convey information about speed. In 83% of cells, fits to the transient or sustained speed tuning curves using the skewed Gaussian were judged as better than simply using a speed-independent constant firing rate ( $P < 0.05$ ).

Response latencies of cells in all areas showed strong speed dependence with median latencies at high speeds significantly shorter than latencies at the lower speeds (Figs. 1 and 2, F–J). No systematic differences in latencies were observed between the different cortical areas or cell types: at each tested speed, there was a large overlap in the latency distributions. Importantly, latencies were discounted for trials in which the response never crossed the response threshold or was already above the threshold at the time of motion onset. One explanation for the speed dependence of latencies is that cells have

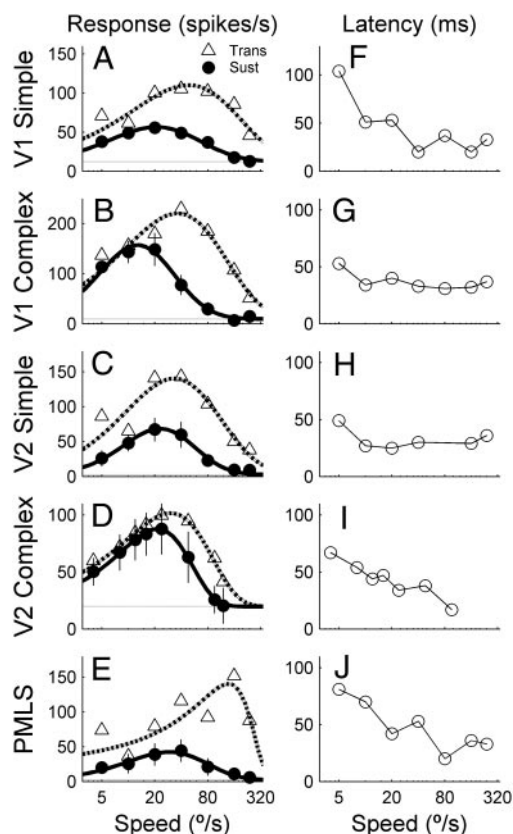


FIG. 2. Transient and sustained responses to speed steps (A–E) and the corresponding latencies for each speed (F–J), shown for the 5 cells the SDFs of which are presented in Fig. 1. Scales on the abscissa are the same in each plot. In A–E, error bars show the SD across trials for the sustained responses and curves show the best-fit skewed-Gaussian. Latencies are not shown for trials in which the response never became significant or was already above the threshold at the time of motion onset.

fixed response latencies, but their responses are only initiated after the stimulus has moved a fixed distance. Thus for each cell's responses we fitted the function:  $L(v) = L_0 + s_0/v$  where  $L(v)$  is the response latency for a stimulus with velocity  $v$ ;  $L_0$  is the cell's stimulus-independent latency; and  $s_0$  is the minimum stimulus displacement before the cell responds.

Across the population of cells, the median  $R^2$  value for these fits was 0.53 (25th and 75th percentiles 0.16 and 0.85), indicating that this function provides reasonable fits for the majority of cells. The median values of  $L_0$  and  $s_0$  were 35 ms and  $0.24^\circ$  for the population of cells with  $R^2$  values  $>0.5$ . This indicates that across the population, the speed dependence of latency probably arises because cells require a stimulus to move  $\geq 0.24^\circ$  before responding (the time to do so being inversely related to speed) and then have a fixed stimulus-independent latency of 35 ms added to that value.

If the  $R^2$  value of the skewed Gaussian fit was  $>0.75$  and the  $F$  test judged the fit better than using constant firing rate, the preferred speed and corresponding peak response amplitude for each cell were recorded from the parameters of the fit. If the fit was inadequate, the preferred speed was simply assigned as the test speed evoking the largest response. Figure 3A compares the preferred speeds from transient and sustained responses for all cells across all areas. Preferred speeds of transient responses were significantly higher than those of sustained responses ( $P < 0.05$ , Student's  $t$ -test), except for V2 simple cells (Fig. 3B). There was significant scatter in the range of preferred speeds across the population of cells and the two measures of preferred speed were poorly correlated ( $R^2 < 0.35$ ) for all cell types other than V1 simple cells for which the  $R^2$  value was 0.70. Figure 3B shows the median preferred speed for each cell type, with error bars showing the 25th and 75th percentiles. Complex cells tend to have higher preferred speeds than simple cells, and PMLS cells tend to have higher preferred speeds than V1 and V2 cells.

To assess the adaptation of each cell's responses, we initially compared the peak response amplitude of the transient and sustained responses measured at each component's preferred speed (Fig. 4A). Across all cell types, the median ratio of transient to sustained responses was 4.1 with transient responses consistently significantly larger than sustained responses. This in itself is not surprising because the transient responses represent a peak firing rate calculated in a short time window while the sustained responses are averaged over a longer period. However, except for simple cells, the two response amplitudes were generally poorly correlated with  $R^2$  values for the five cell types of: V1 simple, 0.46; V1 complex, 0.08; V2 simple, 0.87; V2 complex, 0.01; and PMLS, 0.22. Highly transient responses were observed for the majority of cells in all regions, as demonstrated by the large disparity between the median response amplitudes in Fig. 4B.

The simplicity of the transient-sustained response ratio makes it an attractive measure for quantifying the level of adaptation (e.g., Lisberger and Movshon 1999; Maddess et al. 1988). However, this ratio leads to very large or infinite values if the sustained response amplitude and spontaneous firing rate are similar, and it does not consider the speed dependence of adaptation. To avoid these problems, we calculated a transient-sustained contrast ratio at each stimulus speed:  $TS_{\text{contrast}}(s) = [R_{\text{Trans}}(s) - R_{\text{Sust}}(s)] / [R_{\text{Trans}}(s) + R_{\text{Sust}}(s)]$ , where the transient and sustained responses  $R_{\text{Trans}}$  and  $R_{\text{Sust}}$  are expressed

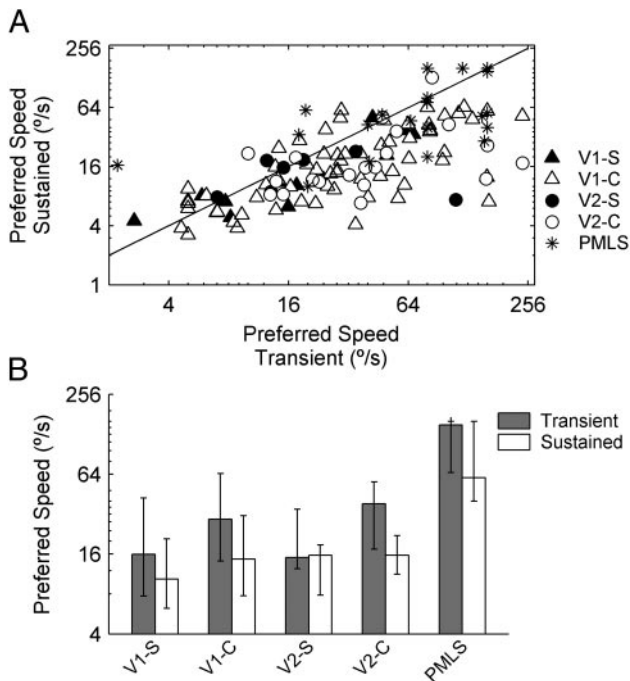


FIG. 3. Population summary of preferred speeds. *A*: comparison of the preferred speeds measured using transient and sustained responses, shown for each cell type. *B*: median preferred speeds measured using transient and sustained responses, shown for each cell type. Error bars show 25th and 75th percentiles in preferred speed distribution.

relative to the spontaneous firing rate. Values of  $TS_{\text{contrast}}$  close to 0 indicate that no adaptation occurred, as the transient and sustained responses are similar. As values of  $TS_{\text{contrast}}$  increase  $>0$ , they indicate greater levels of adaptation. Values  $>1$  indicate that the sustained response is suppressed below the spontaneous firing level. Figure 4C shows the median of  $TS_{\text{contrast}}$  calculated for each cell type and for stimulus speeds of 5–240°/s. At low speeds, contrast ratios for cells in all regions are close to 0.5, demonstrating the similar level of adaptation in all cell types. As speed increases the value of the contrast ratio increases for all regions, although this effect is smaller in PMLS (\*). Thus at higher speeds, the cell responses become increasingly transient, indicating a higher level of adaptation. Importantly, whereas the rate of adaptation is speed dependent, the cell's sustained responses remain speed tuned, indicating that the cells are responding to stimulus speed and not simply fixed displacements.

#### Responses to accelerations and decelerations

We compared the responses of cells to speed profiles comprising linear acceleration from 0°/s to a plateau speed of 120 or 240°/s, then linear deceleration to 0°/s at the same rate as the acceleration period. The aim of using high plateau speeds was to ensure that the cell's preferred speed was included in the range of the speed ramp. Figure 5 shows the SDFs associated with speed ramp rates of 30–2,400°/s<sup>2</sup> for the same five cells shown in Fig. 1. The plateau speeds were 120°/s for the V2 complex cell and 240°/s for all other cells. For comparison, the response to a step change to the plateau speed is also shown (*top graphs*).

A problem associated with comparing the response profiles for different ramp rates is that they have different durations. To

overcome this, we compared the responses to speed ramps using units of speed on the abscissa, rather than time, by transforming the stimulus time to represent the instantaneous stimulus speed. Because all stimuli covered the same speed range, the responses to different ramps spanned the same speed range on the abscissa. When plotted in this way (not shown), response profiles across the range of acceleration and deceleration rates were clearly different. Further, in almost all cells, the acceleration responses were different to the speed tuning curves measured using the responses to speed steps (Fig. 2). This demonstrates that the responses to acceleration are not simply a read-out of a cell's speed tuning curves. Importantly, the shapes of the SDFs did not vary systematically with changes in the acceleration or deceleration rate. However, comparison of the responses to acceleration and deceleration of the same rate shows that the peak and average spiking rates are typically higher for the responses to acceleration than deceleration.

To quantify the responses to speed ramps, we used similar transient and sustained measures of spiking rate to those used for responses to speed steps (see METHODS). The transient ( $\blacktriangle$ , acceleration;  $\triangle$ , deceleration) and sustained ( $\bullet$ ,  $\circ$ ) responses of each cell are shown as *insets* above their SDFs (Fig. 5). These responses suggest that there is no clear acceleration tuning in the cells. That is, responses were not maximal for one partic-

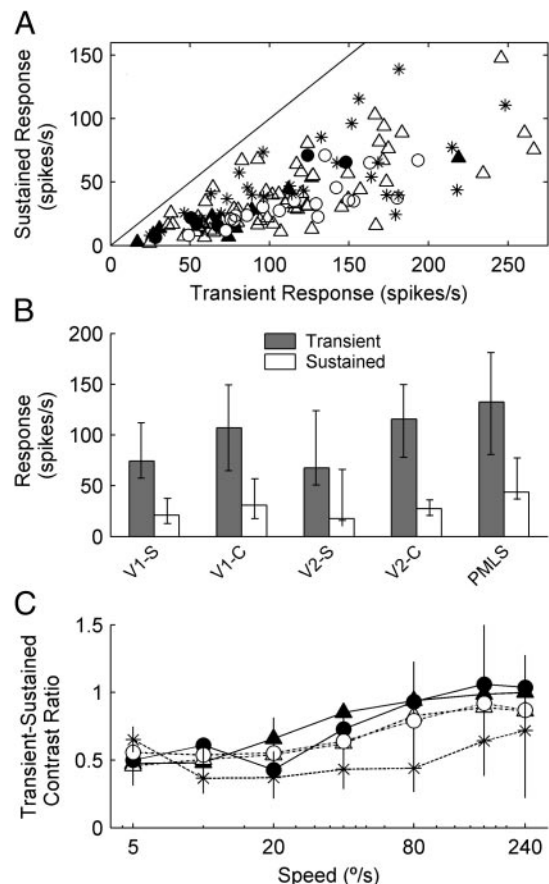


FIG. 4. *A*: transient and sustained response amplitudes measured at each cell's preferred speed shown for all cell types. Marker conventions as in Fig. 3. *B*: median response amplitudes for each cell type are shown for transient and sustained responses. Error bars show 25th and 75th percentiles. *C*: transient-sustained contrast ratio calculated for each speed and cell type.

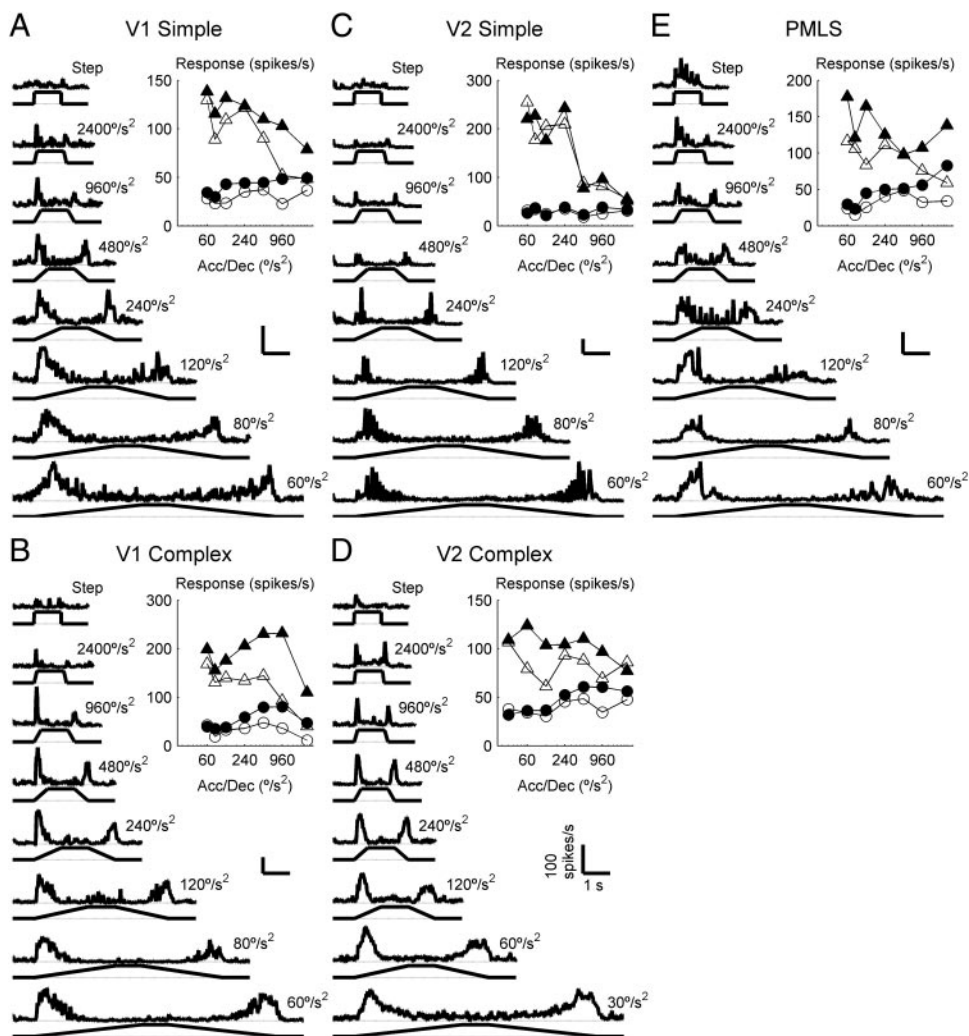


FIG. 5. SDFs produced by speed ramps for the 5 cells shown Figs. 1 and 2. *Insets*: transient ( $\blacktriangle$ , acceleration;  $\triangle$ , deceleration) and sustained ( $\bullet$ , acceleration;  $\circ$ , deceleration) responses to each ramp period. The stimulus speed profiles are shown underneath each SDF.  $\cdots$ ,  $0^\circ/\text{s}^2$ , the plateau speeds were  $120^\circ/\text{s}$  for the V2 complex cell and  $240^\circ/\text{s}$  for all other cells. Vertical and horizontal marker bars in each panel indicate a firing rate of 100 spikes/s and time of 1 s.

ular acceleration with decreased firing rates for lower and higher accelerations. Sustained responses were quite similar across the rates tested, with accelerations evoking progressively larger responses than decelerations as the rate increased. Transient responses to acceleration and deceleration showed greater disparity. This is especially evident for the *V1 complex cell*, which shows large responses to acceleration, but significantly smaller responses to deceleration for the three highest rates tested.

#### Does acceleration tuning exist?

We quantified the level of speed and acceleration tuning present in the population of cells using two measures. First, we assessed the quality of least-squares skewed Gaussian fits to each cell's responses to speed steps (Fig. 2) and speed ramps (Fig. 5). The fits were judged as indicative of speed or acceleration tuning if the fitted  $R^2$  value exceeded 0.75 and an  $F$  test indicated that the skewed Gaussian provided a significantly better fit to the data than a constant firing rate ( $P < 0.05$ ). Responses to speed steps, acceleration and deceleration were considered separately, with only good fits to either a cell's transient or sustained responses needed for the cell to be deemed "tuned." Figure 6A shows the proportion of cells within each cortical area that had good tuning based on the

quality of a skewed Gaussian fit. The majority of cells in all areas showed speed tuning, (V1 simple, 69%; V1 complex, 79%; V2 simple, 100%; V2 complex, 90%; PMLS, 72%), however, never more than 28% of cells in any area showed acceleration or deceleration tuning.

Due to the a priori assumption that a skewed Gaussian was an appropriate fitting function in the previous section, we used a second method to quantify the level of tuning, by looking for systematic variation in the responses to speed steps and ramps. Responses were judged as systematically varying if they showed a clear preferred speed or ramp rate with smaller responses if stimulus speed or ramp rate was increased or decreased. To allow for minor fluctuations in spiking rate, responses were allowed to deviate by  $\leq 20\%$  from monotonicity either side of the preferred speed or ramp rate. Across the five cell types, only 40–75% and 43–58% of cells showed systematic variation in their acceleration and deceleration responses, respectively (Fig. 6B). In comparison, 97% of cells showed systematic response variations to speed steps.

Across the studied population of cells, just 10 were classified as tuned using both measures outlined in the preceding text and testing with a range of accelerations (2 V1 simple cells; 5 V1 complex cells; 2 V2 complex cells, and 1 PMLS cell). Two of these 10 cells, plus an additional 3 cells were classified as

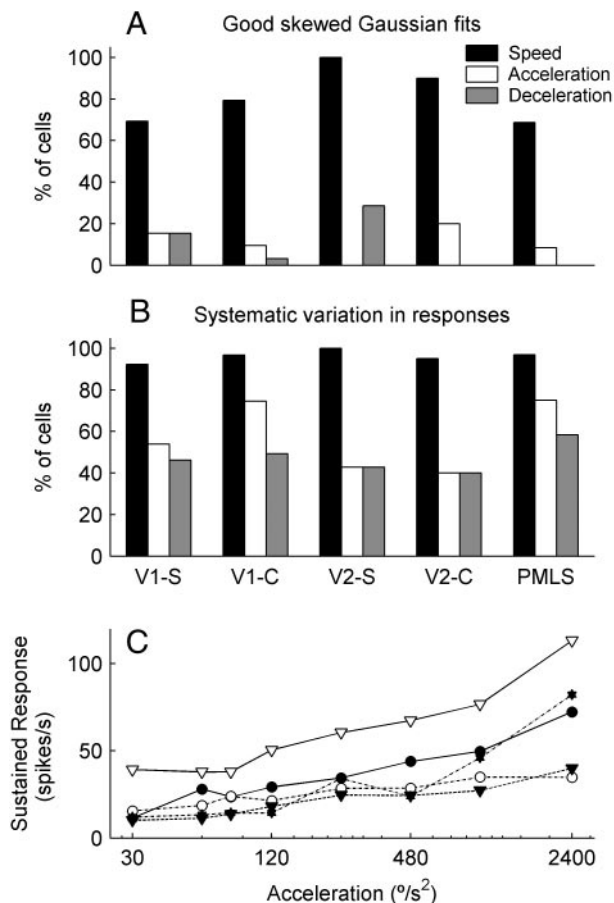


FIG. 6. Proportion of cells showing tuned responses for speed, acceleration and deceleration tests. A cell's responses were judged as tuned based either on the quality of the fit of a skewed Gaussian function (A) or if the responses showed systematic variation across the range of speeds or ramp rates tested (B). C: sustained responses to acceleration for 5 of the 17 cells that had good skewed Gaussian fits.

being tuned when testing with a range of decelerations (2 V1 simple cells; 2 V1 complex cells, and 1 V2 simple cell). We examined these 13 cells in detail and found that the good skewed Gaussian fits and systematic response variation were mainly evident in their sustained responses, which increase monotonically with acceleration. This can be seen in the SDFs and tuning curves shown in Fig. 5. The sustained responses to acceleration are shown for an additional five cells (Fig. 6C). As is evident from the SDFs in Fig. 5, these cells do not respond to the entire range of speeds presented in the ramps. Thus for low ramp rates, there is a large proportion of time during which the firing rate is quite low. Conversely, for high acceleration rates, which have short-duration ramps, the high transient response of the cell dominates the entire period of the motion response, leading to a large response to the ramp. Thus as ramp rate increases, the mean firing rate increases because it is less affected by the periods of time when the cell is unresponsive and the firing rate is low. This indicates that the apparent acceleration tuning evident in the sustained responses to acceleration is most likely a reflection of the cell's speed tuning and the different durations associated with different ramp rates. Thus cells in V1, V2, and PMLS do not show explicit *tuning* to stimulus acceleration.

### Acceleration versus deceleration

Despite the lack of acceleration tuning across the population of cells, it is possible that useful information about instantaneous stimulus speed can still be extracted from stimuli with changing speeds. In the next two sections, the amplitude of responses evoked by acceleration and deceleration are compared and we assess methods by which a cell's preferred speed can be inferred from the responses to speed ramps.

The sustained responses to acceleration and deceleration at  $80^\circ/s^2$  are compared for all cells in Fig. 7A. Clearly, acceleration generates larger responses than the corresponding deceleration in almost all cells. This was quantified at each ramp rate using an acceleration-deceleration tuning index:  $ADTI = (R_{Acc} - R_{Dec}) / (R_{Acc} + R_{Dec})$ , where  $R_{Acc}$  and  $R_{Dec}$  are the transient or sustained responses to acceleration and deceleration. ADTI values close to 0 indicate that acceleration and deceleration produce similar response amplitudes, while values close to 1 or  $-1$  indicate a strong preference for acceleration or deceleration, respectively. Median values of ADTI are shown for cells from each cortical area, plotted separately for transient ( $\Delta$ ) and sustained ( $\bullet$ ) responses (Fig. 7, B-F). All points on the graph except for one (Fig. 7F) show positive ADTI values, indicating that for the majority of cells, acceleration produced larger responses than deceleration. Across the 845 tests of different ramp rates performed on the population of 146 cells, ADTI values were negative for only 11% (transient) and 14% (sustained) of tests. Further, the responses to deceleration become progressively smaller with increasing rate, reflected in the fact that the ADTI increases with ramp rate (Fig. 7).

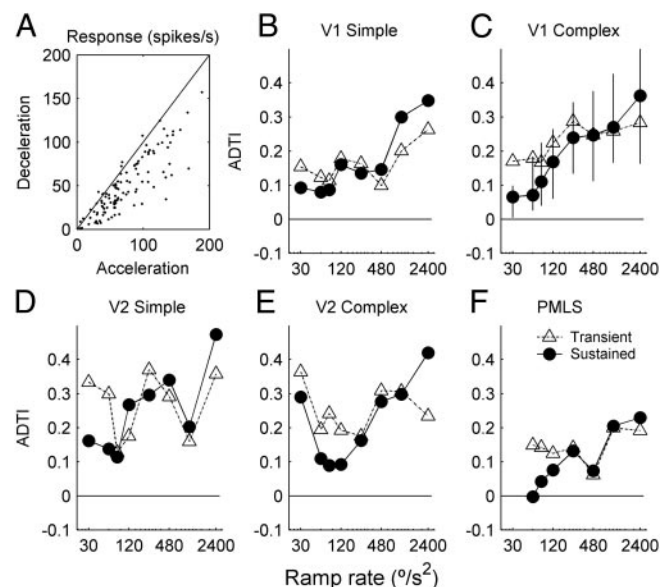


FIG. 7. Comparison of transient and sustained responses to accelerations and decelerations of the same rate. A: scatter plot showing sustained responses of all cells to a  $80^\circ/s^2$  acceleration and deceleration. B-F: acceleration-deceleration tuning index (ADTI) calculated for each ramp rate shown separately for cells of each type and from each brain area. For clarity, error bars indicating 25th and 75th percentiles are only shown for the sustained responses of V1 complex cells. These are representative of the size of the percentile ranges found for other cell types.

### Inferring preferred speeds from acceleration responses

We inferred a cell's preferred speed from its responses to acceleration and deceleration by finding the instantaneous stimulus speed at the time when the firing rate peaked. This time was taken from the center of the transient response window minus the cell's latency associated with a step to its preferred speed. Thus we have four measures of a cell's preferred speed: the speed steps producing the largest transient (1) and sustained (2) responses and the preferred speeds inferred from the responses to acceleration (3) and deceleration (4). Surprisingly, there was poor correlation among all of these measures, regardless of the ramp rate. Figure 8 demonstrates this for accelerations and decelerations of  $240^\circ/\text{s}^2$ . The coefficient of determination between preferred speeds inferred from acceleration and deceleration was  $R^2 = 0.09$  (Fig. 8A).

To demonstrate the fidelity of the method used to infer preferred speeds, the horizontal and vertical error bars in Fig. 8A indicate the SE for preferred speeds estimated from single trials. Further, for each cell we analyzed the response to each stimulus trial individually and calculated the SE of the times of peak firing rate within each stimulus trial. For all cells tested with an accelerating  $240^\circ/\text{s}^2$  ramp, the median SE was 33 ms (25th and 75th percentiles 18 and 47 ms), corresponding to an

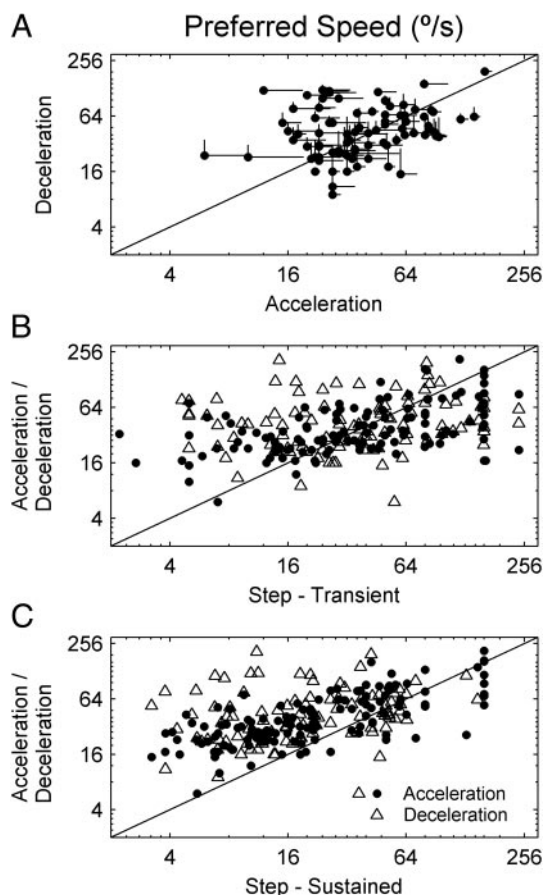


FIG. 8. Comparison of preferred speeds measured using speed steps and inferred from the time of peak response to speed ramps of  $240^\circ/\text{s}^2$ . Comparisons are made between the preferred speeds inferred from acceleration and deceleration tests (A), the preferred speed calculated from the transient response to speed steps and from speed ramps (B), and the preferred speed calculated from the sustained response to speed steps and from speed ramps (C).

error in the inferred speed of  $8^\circ/\text{s}$ . Similarly, for cells tested with a decelerating  $240^\circ/\text{s}^2$  ramp, the median SE was 50 ms (25th and 75th percentiles 39 and 81 ms), corresponding to a speed error of  $12^\circ/\text{s}$ . These time and speed errors are small compared with the 1-s duration of the  $240^\circ/\text{s}^2$  ramp, demonstrating the reliability of the method used to infer preferred speed.

The preferred speeds measured using the transient response to speed steps were also poorly correlated with the preferred speeds inferred from acceleration and deceleration (Fig. 8B:  $R^2 = 0.16$  for acceleration;  $R^2 = 0.02$  for deceleration). A significant finding was that preferred speeds inferred from ramps were significantly higher ( $P < 0.001$ ) than those measured using the sustained response to speed steps (Fig. 8C). Despite this, the preferred speed measures were poorly correlated ( $R^2 = 0.35$  for acceleration;  $R^2 = 0.09$  for deceleration). This suggests that the responses to speed ramps cannot be used to predict a cell's preferred speed and vice versa.

For each cell type we calculated the median preferred speed at each acceleration and deceleration rate (Fig. 9, A and B). Notably, PMLS cells (\*) tend to have the highest preferred speeds while V1 simple cells (<97) tend to have the lowest. This is consistent with the findings for preferred speeds measured from responses to speed steps (Fig. 3). Two extremes in the dependence of preferred speed on ramp rate and the time of peak spiking rate could be expected. First if cells have a fixed preferred speed that is independent of the ramp rate, then the time of the peak response should decrease with increasing ramp rate. Second, if the peak response occurs at a fixed time after ramp onset, then the preferred speed should increase with increasing ramp rate. Instead, responses showed behavior with both characteristics. For all cell types, the preferred speeds increase with increasing ramp rate (Fig. 9, A and B). This is not simply due to the cell's peak response occurring at a fixed latency after ramp onset, as highlighted in Fig. 9, C and D, which plots the time of the peak response relative to the time when the ramp speed is  $0^\circ/\text{s}$  (i.e., the onset of acceleration or end of deceleration). Importantly, the peak times are not fixed, but decrease with increasing rate. The increase in preferred speeds with ramp rate suggests that the peak firing rate occurs progressively later in time for acceleration tests and progressively earlier in time for deceleration tests than would be expected from the responses to the lowest acceleration rate.

A possible explanation for the change in preferred speed with ramp rate is that the response latencies may have been consistently under- or overestimated. The time at which response rate peaks is adjusted by the cell's latency to find the instantaneous stimulus speed that "caused" the peak in firing rate. Consequently, the calculation of latency is crucial, especially at higher ramp rates. For example, a latency error of 20 ms leads to a speed error of  $1.2^\circ/\text{s}$  for a  $60^\circ/\text{s}^2$  acceleration but an error of  $48^\circ/\text{s}$  for a  $2,400^\circ/\text{s}^2$  acceleration. Underestimating latency should lead to overestimates of the preferred speed for acceleration. Because these overestimates become more significant with increasing acceleration rate, this matches the trend of increasing preferred speeds we observed (Fig. 9A). However, applying the same underestimated latencies to deceleration should lead to increasing underestimates of preferred speed with increasing rate, which does not match the trend seen in Fig. 9B. Thus it is unlikely that latency calculations are the source of the rate dependence of the preferred speeds.

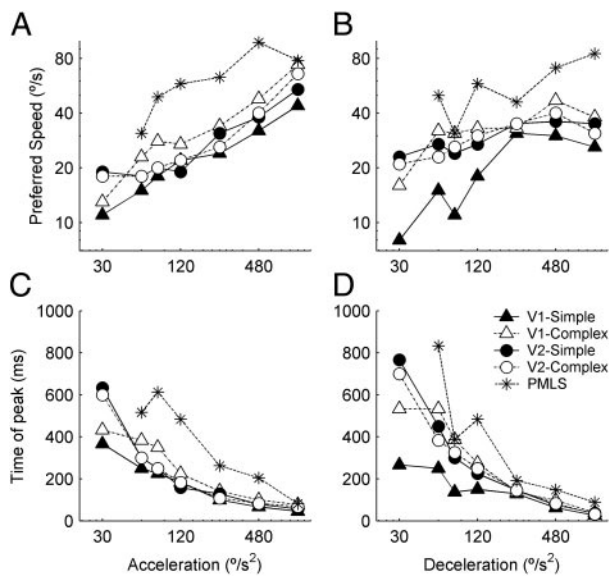


FIG. 9. Median preferred speeds for each cell type, inferred from the stimulus speed at the latency adjusted time of the peak response to accelerations (A) and decelerations (B) of 30–2,400 $^{\circ}/s^2$ . The corresponding time at which the response peaks is shown, calculated relative to when the stimulus speed reaches 0 $^{\circ}/s$  (C and D). For accelerations (C), times are relative to the onset of motion. For decelerations (D), times are relative to the cessation of motion.

## DISCUSSION

In the INTRODUCTION, we posed the question of how the visual system addresses the problem of coding changes in speed. Three possibilities were suggested. First, neurons might display acceleration tuning in the same way that motion-sensitive neurons are speed tuned. Our data show conclusively that this is not the case. As outlined in the following text, the difficulties in coding speed changes in the cat cortex appear to mirror human psychophysical sensitivity to acceleration. Second, adaptation might degrade a neuron's ability to accurately code constant speeds and changes in speed. Our data demonstrate that adaptation alters speed tuning properties and influences the way in which acceleration and deceleration at the same rate are coded. Third, while not explicitly coding stimulus acceleration, a neuron's responses could be decoded to reliably estimate stimulus speed and acceleration if the influence of adaptation is quantified. Our present data are consistent with a previous model of acceleration responses in macaque MT showing that if adaptation is incorporated, it can be used to decode the responses to acceleration (Price et al. 2005). However, as outlined in the following text, the present data demonstrate that the firing-rate-dependent adaptation in that model may not be entirely appropriate for decoding signals in neurons where adaptation depends on multiple stimulus parameters.

### Speed tuning but not acceleration tuning

We studied the responses of motion-sensitive neurons in cortical areas V1, V2, and PMLS in the anesthetized cat using steps and ramps in stimulus speed. The majority of cells displayed speed tuning, characterized by a clear preferred speed. The existence of speed tuning in these cells, as determined using moving texture and aperiodic patterns has been demonstrated previously (Casanova et al. 1995; Hamada 1987;

Merabet et al. 1997). We found higher preferred speeds in V1 and V2 than previous studies and also that preferred speeds in the two areas were similar. These differences with earlier reports may relate to the large texture elements used in our stimuli (0.8 $^{\circ}$ ) compared with previous reports (e.g., 0.04–0.64 $^{\circ}$  in Casanova et al. 1995), because a neuron's preferred speed tends to be higher when larger texture elements are used. Technically, when tested with spatial sine-wave gratings, cells in V1, V2, and PMLS do not always show speed tuning but are tuned to the spatial or temporal frequencies contained within a stimulus (Morrone et al. 1986; Movshon et al. 1978; Zumbroich and Blakemore 1987). Although many cells only respond to a narrow range of spatial frequencies, they should still be stimulated by our stimuli, which contain a broad range of spatial frequencies. One problem with broadband stimuli, discussed further in the following text, is that it can be difficult to disambiguate the different effects of spatial and temporal frequency on adaptation (Saul and Cynader 1989a,b).

The present study is the first to assess the responses of neurons in feline cortex to the gradual speed changes associated with linear acceleration and deceleration. Unlike their clear speed tuning, we found no strong evidence for acceleration tuning in individual neurons in any of the areas tested. This is evidenced by the lack of a clear preferred acceleration in most cells and the lack of systematic variation in response magnitude as the ramp acceleration or deceleration was varied. Further, apparently systematic changes in neuronal response with ramp rate that are suggestive of acceleration tuning are attributable to a cell's speed tuning and the different stimulus durations associated with different ramp rates. Whereas a simple winner-take-all or population-vector model could determine the stimulus direction and speed from the responses of a population of neurons from these areas, a similar model could not determine the stimulus acceleration because the responses of individual neurons do not vary systematically with acceleration. This suggests that if acceleration is required by later components of the visual or motor system, it must be calculated either by continuously differentiating the population's velocity signal (Price et al. 2005) or by simply comparing stimulus velocities at two points in time.

PMLS is a cortical region thought to be involved in global motion analysis to determine heading direction and guide locomotion (e.g., Brosseau-Lachaine et al. 2001; Kim et al. 1997; Rauschecker 1988). It has been suggested to be roughly homologous and serve a similar functional role to area MT in primates (Payne 1993). Area MT is a specialized motion-processing region involved in the perception of motion (Britten et al. 1992; Nichols and Newsome 2002) and analysis of motion for controlling eye movements (Lisberger et al. 1987). The lack of acceleration tuning in PMLS matches results from studies in MT, which failed to find evidence of acceleration tuning (Lisberger and Movshon 1999; Price et al. 2005). Given the reciprocal anatomical connections among V1, V2 and PMLS (Norita et al. 1996; Sherk 1986) and the fact that motion processing is performed synchronously in these brain areas (Dinse and Kruger 1994; Katsuyama et al. 1996; Vajda et al. 2000), it is logical that we found little evidence for acceleration tuning in V1 and V2.

The lack of evidence for acceleration tuning in macaque MT and cat V1, V2, and PMLS supports psychophysical findings that have failed to find evidence for specific acceleration

sensitivity in humans (Snowden and Braddick 1991; Werkhoven et al. 1992). Although subjects are sensitive to speed differences as small as 5% between sequentially presented stimuli (McKee 1981), the ability to detect gradual changes in speed is quite poor (Schmerler 1976; Werkhoven et al. 1992). Thus acceleration and deceleration are most likely detected perceptually by comparing stimulus speeds at two points in time (Brouwer et al. 2002; Watamaniuk and Heinen 2003) rather than by ongoing differentiation of the speed signal. In the macaque, MT provides motion analysis for the control of eye movements and perception of motion. Acceleration sensitivity is not evident perceptually in humans, but in the macaque is evident in regions involved in eye-movement control, which receive inputs from MT. This suggests that this sensitivity to visual acceleration must arise after the motion processing performed by MT.

### *Influence of adaptation*

Despite the lack of evidence for specific acceleration tuning in the areas studied, we found clear differences in the responses of individual neurons to acceleration and deceleration at the same rate. Both the transient and sustained firing rates evoked by an accelerating stimulus are higher than those evoked by the corresponding deceleration. These differences are observed across a range of ramp rates with the preference for acceleration increasing with rate. The cause of these differences is probably that adaptation reduces the cell's responsiveness rather than differential coding of acceleration and deceleration. Given the impact of adaptation, the fact that deceleration tests always followed periods of acceleration and constant speed suggests that deceleration responses should be smaller than the responses to the preceding acceleration. This finding strongly demonstrates the importance of adaptation in altering the coding of speed and speed changes. The role of this adaptation may be to maximize a cell's ability to transfer information about stimulus motion by centering that part of a cell's speed tuning function, which shows maximal changes in spike rate with changes in speed, on the prevailing mean stimulus speed (Ibbotson 2005a,b). Thus the cell would be maximally sensitive to speed changes at speeds close to those to which it has been adapted. A similar functional role for adaptation has been demonstrated in motion sensitive neurons in the fly (Brenner et al. 2000; Fairhall et al. 2001).

The rate dependence of the acceleration-deceleration tuning index (ADTI) can also be explained by rapid adaptation of neural sensitivity. For low rates of acceleration and deceleration, neurons will be affected by adaptation while they are responding to the early component of the acceleration stimulus. Thus adaptation similarly affects responses to acceleration and the subsequent deceleration, resulting in low ADTI values. For higher rates, adaptation will have a smaller effect on responses to acceleration because the period of motion is so short. However, the period of constant speed stimulation ensures a relatively large effect on responses to deceleration, causing a greater disparity between acceleration and deceleration responses and higher ADTI values.

Adaptation clearly affects the way in which individual neurons code stimulus speed. This is evident from the transient nature of the responses to speed steps and the lack of correlation between the preferred speeds calculated from the re-

sponses to speed steps and speed ramps. Two factors make it difficult to reliably and accurately use the responses to speed steps to predict the responses to speed ramps or vice versa. First response latencies are strongly speed dependent, with low speeds having significantly longer response latencies than high speeds. This suggests that we may see response "compression" associated with the responses to acceleration because the long-latency responses to the initially presented low speeds will overlap the responses to subsequently presented high speeds. Similarly, response "dispersion" may be associated with deceleration, since high speeds have shorter latencies than subsequently presented low speeds.

A second factor affecting response predictions is the stimulus dependence of a neuron's adaptation rate. The neuron's adaptation rate depends critically on the temporal frequency of the stimulus, most often being maximal at optimal or higher than optimal temporal frequencies (Ibbotson et al. 1998; Maddess et al. 1988). Moreover, adaptive changes to a neuron's temporal and spatial tuning properties exhibit both temporal and spatial frequency-selective mechanisms (Saul and Cynader 1989a,b). Saul and Cynader demonstrated that adaptation tends to produce repulsive shifts in the preferred spatial and temporal frequencies of neurons in cat striate cortex. Thus adaptation at a high temporal frequency tends to shift the neuron's preferred temporal frequency to lower values. Further, they showed that adaptation is most evident in cells tested with higher temporal frequencies and lower spatial frequencies than a given cell's preferred stimulus. This supports our findings that adaptation is more rapid and stronger at high speeds, as indicated by the speed dependence of the transient-sustained contrast ratio. Based on this, we would expect adaptation effects to be strongest *late* in the responses to an accelerating stimulus, but evident *early* to a decelerating stimulus.

### *Comparing preferred speeds*

In an attempt to measure if the system retained a unique speed tuning profile at all levels of adaptation, we assessed the preferred speeds of neurons using four measures. These were the speed step for which a neuron gave the largest transient (1) and sustained (2) response and the stimulus speed that generated the largest response during acceleration (3) and deceleration (4). All measures were poorly correlated, reflecting the confounding effects of adaptation. Examination of the SDFs associated with speed steps demonstrates that it is not surprising that preferred speeds for transient and sustained measures are poorly correlated. At high speeds, most cells give large, brisk onset responses to motion but are often then entirely unresponsive to continuing motion. Due to the brief motion-onset responses, the transient speed tuning curves of neurons often appear as high-pass functions, indicating much higher preferred speeds than those calculated using the sustained speed tuning curves. This suggests that adaptation impairs the interpretation of the responses to a constant sustained stimulus in addition to the problems associated with a stimulus in which speed is changing. The rapid adaptation associated with responses to motion onset mean that across the cell population it is not unexpected that the transient preferred speed is poorly correlated with preferred speeds inferred from responses to acceleration/deceleration.

Interestingly, the preferred speeds inferred from the responses to acceleration and deceleration were significantly higher than those associated with the sustained responses to speed steps. This may be attributable to the large proportion of time spent at high stimulus speeds because the ramps peaked at speeds of 120 or 240°/s, which are considerably higher than the preferred speeds of most neurons. Thus speeds similar to the preferred speed measured using speed steps are presented for relatively short periods of time. A potential solution to this problem would be to use ramps with logarithmic changes in speed. Thus each octave in speeds would be represented for the same duration of time.

A more likely explanation of the higher preferred speeds measured using speed ramps is that adaptation during the speed ramps systematically increases the preferred speed of the cells. Similar effects of adaptation altering a neuron's preferred speed have been reported previously in motion-sensitive neurons of the subcortical nucleus of the optic tract (Ibbotson 2005a; Ibbotson et al. 1998) and V1 neurons in the cat (Saul and Cynader 1989b). This emphasizes the probability that adaptation mechanisms may severely confound the responses to speed ramps such that judgements of the current stimulus speed are impaired. Such impairments of speed judgements have been shown in psychophysical studies, in which human observers have difficulty in detecting slow accelerations and also severely underestimate the ratio of start and end speeds associated with periods of acceleration and deceleration (Schmerler 1976).

#### *Models of acceleration and adaptation coding*

Previous models used to describe the responses to stepped and ramped speed changes have not explicitly taken into account speed-dependent variations in both response latency and adaptation rate; however, they have successfully reproduced most of the temporal response characteristics of speed- and acceleration-sensitive neurons (Lisberger and Movshon 1999; Price et al. 2005; Zhang et al. 2005). The model developed by Lisberger and Movshon (1999) incorporates the speed dependence of response latency but not adaptation. Instead, by weighting responses relative to the transient and sustained motion responses, it can neatly fit the responses to a range of stimuli incorporating sinusoidal, stepped and ramped speed variations. Importantly, preferred speeds were not inferred from acceleration and deceleration responses in previous studies (Lisberger and Movshon 1999; Zhang et al. 2005), thus it is difficult to assess if these models accurately captured the timing of the peak response during presentation of speed ramps. Interestingly, Lisberger and Movshon argued that the firing of an MT neuron is only likely to be influenced by acceleration if the initial stimulus speed is close to zero or well below the neuron's preferred speed. Our data suggest that neuronal adaptation is stimulus-dependent, thus the entire stimulus history including the full range of speeds presented and their duration can affect a neuron's future response to motion, including any impact of acceleration.

We have previously studied the effects of adaptation on the responses of MT neurons in alert macaques to acceleration (Price et al. 2005). While individual neurons did not explicitly code visual acceleration, responses to a given acceleration rate were typically higher than those evoked by the corresponding

deceleration of the same rate. Further, a neuron's responses to acceleration were not well predicted by their speed tuning, calculated from transient and sustained responses to constant steps in stimulus speed. From this, we developed a model incorporating adaptation and a neuron's speed tuning that could predict the responses to acceleration. This suggested that adaptation mechanisms can explain the different responses evoked by a range of acceleration and deceleration rates. Importantly, this model was able to account for the change in timing of the peak responses and associated changes in inferred preferred speed determined from a range of acceleration and deceleration rates. The strong similarity between the physiological responses to acceleration in cat cortex and macaque MT suggests that the adaptive model used in MT could simulate many of the response properties observed in the cat cortical neurons.

However, the model used for monkey MT only incorporated a spike-rate-dependent adaptation mechanism. Firing-rate-dependent adaptation, also known as neural fatigue, is unlikely to solely account for the different responses to the range of tests conducted in the cat cortex because adaptation strength is not related to firing rate in cat V1 (Vidyasagar 1990). This is evident in the present data because the sustained responses to speed steps are still speed tuned and adaptation occurs even for stimuli that do not evoke high firing rates. Some of the response decline that we observed can be attributed to contrast adaptation. Exposure to high-contrast stimuli reduces the responses of magnocellular cells in the macaque LGN and in most cells of macaque and cat striate cortex (Ohzawa et al. 1982; Solomon et al. 2004), an effect partially associated with the hyperpolarization of the membrane potential and increased membrane conductance of the adapting cells (Sanchez-Vives et al. 2000). Synaptic depression has also been shown to affect V1 cells with time constants of both tens and hundreds of milliseconds (Varela et al. 1997). Synaptic depression can perform temporal low-pass filtering, which influences the preferred temporal frequency (and therefore preferred speed) of motion-sensitive neurons (Fortune and Rose 2001). This suggests that changes in synaptic efficacy could account for changes in the low-pass temporal filtering performed by a cell and the associated stimulus-dependent changes in a neuron's preferred temporal frequency.

As outlined in the preceding text, the model used to simulate the monkey MT data can be used to reasonably predict individual cell responses from the cat data and extract acceleration responses from the population of cat cells. However, this is clearly not the final answer. The present paper reveals that future models must also take account of the speed-dependence of adaptation and response latencies, and a multitude of stimulus parameters such as contrast, temporal frequency and spatial frequency may all have inter-related effects on adaptation. Using grating stimuli, it should be possible to study the effects of spatial and temporal frequency on adaptation, which was precluded by our use of spatially broadband stimuli. Taking these things into account, it might be possible to understand if neurons are able to accurately signal stimulus parameters despite the confounding effects of a changing stimulus and changing neural sensitivity.

## ACKNOWLEDGMENTS

Thanks to Prof. Bogdan Dreher, Drs. Colin Clifford and Szonya Durant, and to S. Wilson for help during recording sessions. Prof. Dreher gave invaluable assistance in recording from V2 and PMLS. Exceptional animal care was provided by K. Debono, K. Wall, and the late R. Cameron.

Present address of N.S.C. Price: Department of Neurobiology, Harvard Medical School, Boston, Massachusetts 02115.

## GRANTS

This work was supported by grants to M. R. Ibbotson from the National Health and Medical Research Council of Australia (224263) and the Institutes of Advanced Studies and to N. A. Crowder from the National Science and Engineering Research Council of Canada.

## REFERENCES

- Albrecht DG, Farrar SB, and Hamilton DB.** Spatial contrast adaptation characteristics of neurons recorded in the cat's visual cortex. *J Physiol* 347: 713–739, 1984.
- Barlow HB and Hill RM.** Evidence for a physiological explanation of the waterfall phenomenon and figural after effects. *Nature* 200: 1345–1347, 1963.
- Bex PJ, Bedingham S, and Hammett ST.** Apparent speed and speed sensitivity during adaptation to motion. *J Opt Soc Am A* 16: 2817–2824, 1999.
- Bonds AB.** Temporal dynamics of contrast gain in single cells of the cat striate cortex. *Vis Neurosci* 6: 239–255, 1991.
- Brenner N, Bialek W, and de Ruyter van Steveninck RR.** Adaptive rescaling maximizes information transmission. *Neuron* 26: 695–702, 2000.
- Britten KH, Shadlen MN, Newsome WT, and Movshon JA.** The analysis of visual motion: a comparison of neuronal and psychophysical performance. *J Neurosci* 12: 4745–4765, 1992.
- Brosseau-Lachaine O, Faubert J, and Casanova C.** Functional sub-regions for optic flow processing in the posteromedial lateral suprasylvian cortex of the cat. *Cereb Cortex* 11: 989–1001, 2001.
- Brouwer AM, Brenner E, and Smeets JBJ.** Perception of acceleration with short presentation times: can acceleration be used in interception? *Percept Psychophys* 64: 1160–1168, 2002.
- Cao P, Gu Y, and Wang S-R.** Visual neurons in the pigeon brain encode the acceleration of stimulus motion. *J Neurosci* 24: 7690–7698, 2004.
- Casanova C, Savard T, Nordmann JP, Molotchnikoff S, and Minville K.** Comparison of the responses to moving texture patterns of simple and complex cells in the cats area 17. *J Neurophysiol* 74: 1271–1286, 1995.
- Das VE, Economides JR, Ono S, and Mustari MJ.** Information processing by parafoveal cells in the primate nucleus of the optic tract. *Exp Brain Res* 140: 301–310, 2001.
- Dinse HR and Kruger K.** The timing of processing along the visual pathway in the cat. *Neuroreport* 5: 893–897, 1994.
- Fairhall AL, Lewen GD, Bialek W, and de Ruyter van Steveninck RR.** Efficiency and ambiguity in an adaptive neural code. *Nature* 412: 787–792, 2001.
- Fortune ES and Rose GJ.** Short-term synaptic plasticity as a temporal filter. *Trends Neurosci* 24: 381–385, 2001.
- Giaschi D, Douglas R, Marlin S, and Cynader M.** The time course of direction-selective adaptation in simple and complex cells in cat striate cortex. *J Neurophysiol* 70: 2024–2034, 1993.
- Hamada T.** Neural response to the motion of textures in the lateral suprasylvian area of cats. *Behav Brain Res* 25: 175–185, 1987.
- Ibbotson MR.** Contrast and temporal frequency related adaptation in the pretectal nucleus of the optic tract. *J Neurophysiol* 94: 136–146, 2005a.
- Ibbotson MR.** Physiological mechanisms of adaptation in the visual system. In: *Fitting the Mind to the World*, edited by Clifford CWG and Rhodes G. Oxford, UK: Oxford Univ. Press, 2005b, p. 17–45.
- Ibbotson MR, Clifford CWG, and Mark RF.** Adaptation to visual motion in directional neurons of the nucleus of the optic tract. *J Neurophysiol* 79: 1481–1493, 1998.
- Ibbotson MR, Price NS, and Crowder NA.** On the division of cortical cells into simple and complex types: a comparative viewpoint. *J Neurophysiol* 93: 3699–3702, 2005.
- Katsuyama N, Tsumoto T, Sato H, Fukuda M, and Hata Y.** Lateral suprasylvian visual cortex is activated earlier than or synchronously with primary visual cortex in the cat. *Neurosci Res* 24: 431–435, 1996.
- Keck MJ and Pentz B.** Recovery from adaptation to moving gratings. *Perception* 6: 719–725, 1977.
- Kim JN, Mulligan K, and Sherk H.** Simulated optic flow and extrastriate cortex. I. Optic flow versus texture. *J Neurophysiol* 77: 554–561, 1997.
- Krauzlis RJ and Lisberger SG.** Temporal properties of visual motion signals for the initiation of smooth pursuit eye movements in monkeys. *J Neurophysiol* 72: 150–162, 1994.
- Lisberger SG, Morris EJ, and Tychsen L.** Visual motion processing and sensory-motor integration for smooth pursuit eye movements. *Annu Rev Neurosci* 10: 97–129, 1987.
- Lisberger SG and Movshon JA.** Visual motion analysis for pursuit eye movements in area MT of macaque monkeys. *J Neurosci* 19: 2224–2246, 1999.
- Lorenceau J.** Recovery from contrast adaptation: effects of spatial and temporal frequency. *Vision Res* 27: 2185–2191, 1987.
- Maddess T, McCourt ME, Blakeslee B, and Cunningham RB.** Factors governing the adaptation of cells in area-17 of the cat visual cortex. *Biol Cybern* 59: 229–236, 1988.
- Maunsell JH and Gibson JR.** Visual response latencies in striate cortex of the macaque monkey. *J Neurophysiol* 68: 1332–1344, 1992.
- McKee SP.** A local mechanism for differential velocity detection. *Vision Res* 21: 491–500, 1981.
- Merabet L, Minville K, and Casanova C.** Modulatory influence of a moving texture background on responses of cells in the cat's postero-medial lateral suprasylvian (PMLS) cortex. *Invest Ophthalmol Vis Sci* 38: 2915–2915, 1997.
- Merabet L, Minville K, Pito M, and Casanova C.** Responses of neurons in the cat posteromedial lateral suprasylvian cortex to moving texture patterns. *Neuroscience* 97: 611–623, 2000.
- Morrone MC, Di Stefano M, and Burr DC.** Spatial and temporal properties of neurons of the lateral suprasylvian cortex of the cat. *J Neurophysiol* 56: 969–986, 1986.
- Movshon JA.** The velocity tuning of single units in cat striate cortex. *J Physiol* 249: 445–468, 1975.
- Movshon JA, Thompson ID, and Tolhurst DJ.** Spatial and temporal contrast sensitivity of neurones in areas 17 and 18 of the cat's visual cortex. *J Physiol* 283: 101–120, 1978.
- Nichols MJ and Newsome WT.** Middle temporal visual area microstimulation influences veridical judgments of motion direction. *J Neurosci* 22: 9530–9540, 2002.
- Norita M, Kase M, Hoshino K, Meguro R, Funaki S, Hirano S, and McHaffie JG.** Extrinsic and intrinsic connections of the cat's lateral suprasylvian visual area. *Prog Brain Res* 112: 231–250, 1996.
- Ohzawa I, Sclar G, and Freeman RD.** Contrast gain control in the cat visual cortex. *Nature* 298: 266–268, 1982.
- Ohzawa I, Sclar G, and Freeman RD.** Contrast gain control in the cat's visual system. *J Neurophysiol* 54: 651–667, 1985.
- Ono S, Das VE, Economides JR, and Mustari MJ.** Modeling of smooth pursuit-related neuronal responses in the DLPN and NRTP of rhesus macaque. *J Neurophysiol* 93: 108–116, 2005.
- Payne BR.** Evidence for visual cortical area homologs in cat and macaque monkey. *Cereb Cortex* 3: 1–25, 1993.
- Petersen SE, Baker JF, and Allman JM.** Direction-specific adaptation in area MT of the owl monkey. *Brain Res* 346: 146–150, 1985.
- Price NSC, Ono S, Mustari MJ, and Ibbotson MR.** Comparing acceleration and speed tuning macaque MT: physiology and modeling. *J Neurophysiol* 94: 3451–3464, 2005.
- Rauschecker JP.** Visual function of the cat's LP/LS subsystem in global motion processing. *Prog Brain Res* 75: 95–108, 1988.
- Sanchez-Vives MV, Nowak LG, and McCormick DA.** Membrane mechanisms underlying contrast adaptation in cat area 17 in vivo. *J Neurosci* 20: 4267–4285, 2000.
- Saul AB and Cynader MS.** Adaptation in single units in visual cortex: the tuning of aftereffects in the spatial domain. *Visual Neurosci* 2: 593–607, 1989a.
- Saul AB and Cynader MS.** Adaptation in single units in visual cortex: the tuning of aftereffects in the temporal domain. *Vis Neurosci* 2: 609–620, 1989b.
- Schmerler J.** The visual perception of accelerated motion. *Perception* 5: 167–185, 1976.
- Sherk H.** Location and connections of visual cortical areas in the cat's suprasylvian sulcus. *J Comp Neurol* 247: 1–31, 1986.

- Skottun BC, De Valois RL, Grosf DH, Movshon JA, Albrecht DG, and Bonds AB.** Classifying simple and complex cells on the basis of response modulation. *Vision Res* 31: 1079–1086, 1991.
- Smith AT.** Velocity coding: evidence from perceived velocity shifts. *Vision Res* 25: 1969–1976, 1985.
- Snowden RJ and Braddick OJ.** The temporal integration and resolution of velocity signals. *Vision Res* 31: 907–914, 1991.
- Solomon SG, Peirce JW, Dhruv NT, and Lennie P.** Profound contrast adaptation early in the visual pathway. *Neuron* 42: 155–162, 2004.
- Suzuki DA, Yamada T, and Yee RD.** Smooth-pursuit eye-movement-related neuronal activity in macaque nucleus reticularis tegmenti pontis. *J Neurophysiol* 89: 2146–2158, 2003.
- Takemura A, Inoue Y, Gomi H, Kawato M, and Kawano K.** Change in neuronal firing patterns in the process of motor command generation for the ocular following response. *J Neurophysiol* 86: 1750–1763, 2001.
- Vajda I, Lankheet MJ, Borghuis BG, and van de Grind WA.** Dynamics of directional selectivity in area 18 and PMLS of the cat. *Cereb Cortex* 14: 759–767, 2004.
- Vajda I, Lankheet MJ, and Huijsman KS.** Summation and integration underlying complex cell receptive fields in cat area PMLS and area 18. *Invest Ophthalmol Vis Sci* 41: S54–S54, 2000.
- Varela JA, Sen K, Gibson J, Fost J, Abbott LF, and Nelson SB.** A quantitative description of short-term plasticity at excitatory synapses in layer 2/3 of rat primary visual cortex. *J Neurosci* 17: 7926–7940, 1997.
- Vautin RG and Berkley MA.** Responses of single cells in cat visual cortex to prolonged stimulus movement: neural correlates of visual aftereffects. *J Neurophysiol* 40: 1051–1065, 1977.
- Vidyasagar TR.** Pattern adaptation in cat visual cortex is a co-operative phenomenon. *Neuroscience* 36: 175–179, 1990.
- Watamaniuk SNJ and Heinen SJ.** Perceptual and oculomotor evidence of limitations on processing accelerating motion. *J. Vision* 3: 698–709, 2003.
- Werkhoven P, Snippe HP, and Toet A.** Visual processing of optic acceleration. *Vision Res* 32: 2313–2329, 1992.
- Zhang C, Wang YJ, and Qi XL.** Modeling the acceleration sensitive neurons in the pigeon optokinetic system. *Biol Cybern* 92: 252–260, 2005.
- Zumbroich TJ and Blakemore C.** Spatial and temporal selectivity in the suprasylvian visual cortex of the cat. *J Neurosci* 7: 482–500, 1987.